Available online at www.sciencedirect.com

jmr&t Journal of Materials Research and Technology

www.jmrt.com.br

Original Article

Mechanical and wear behaviour of nanostructure TiO_2–Ag coating on cobalt chromium alloys by air plasma spray and high velocity oxy-fuel

Mohd Hazwan Hassim, Mohd Hasbullah Idris, Muhamad Azizi Mat Yajid, Syahrullail Samion*

Faculty of Mechanical Engineering, Universiti Teknologi Malaysia, 81310 UTM Skudai, Johor Bahru, Johor, Malaysia

ARTICLE INFO

Article history:
Received 29 August 2018
Accepted 4 April 2019
Available online 4 May 2019

Keywords:
Cobalt–chromium alloy
Nanostructure TiO_2–Ag coating
Thermal spray coating method
Surface properties
Wear performance

ABSTRACT

Cobalt chromium alloys constitutes the base of one important group of biometallic with excellent mechanical properties. However, due to its non-bioactive and non-antimicrobial surface, cobalt chromium alloys are vulnerable to wear corrosive attack and bacterial infection. Hence, coating cobalt chromium alloys surface with superior biomaterials is the best proven techniques. In this work, nanostructure silver adopted titanium dioxide coating was deposited on cobalt chromium alloys using air plasma spray (APS) and high velocity oxy-fuel (HVOF) techniques. Nanostructure TiO_2–Ag coating demonstrated superior hardness, wear resistance and lower coefficient of friction when compared to bare CoCr alloys. Reduced plastic deformation detected by microstructural analysis indicate that the interference of nano-structure coating in metallic matrix help lower the wear rate of the sample. Meanwhile, low porosity of the coating produced by HVOF technique shown a better wear resistance result than APS technique.

1. Introduction

Biomedical implants are used in human body to repair or alter natural human parts [1]. Because of their excellent mechanical properties and acceptable biocompatibility, metallic materials are widely employed as prosthetic devices. Among them, cobalt chromium alloys is the most popular permanent implant material for lower limb application [2]. It is frequently use as an alternative of titanium due to comparable low cost with higher hardness and tensile strength [3]. However, under dynamic human body fluid and repeating load over a long period, this metal suffers fretting corrosion and generates significant concentration of wear ion to the surrounding cell and disseminated throughout the body [4]. With the enhanced early survival of total arthroplasty, long-term implant performance and resistance to wear have been identified as newly-visible challenges [5]. Wear debris-led osteolysis and loosening have therefore been given a ticket as a medium- to long-term concern.

To overcome this problem, the implant should have high wear resistance surface to ensure successful implant-bone adhesion without any interference reaction. Numerous studies have been conducted to modified CoCr alloy surface in order to improve mechanical properties and biocompatibility of the implant [6]. One of the most effective techniques is to coat the implant surface with protective bioactive

* *Corresponding author.*
E-mail: hzwn_sim@yahoo.com (M.H. Hassim).

https://doi.org/10.1016/j.jmrt.2019.04.003

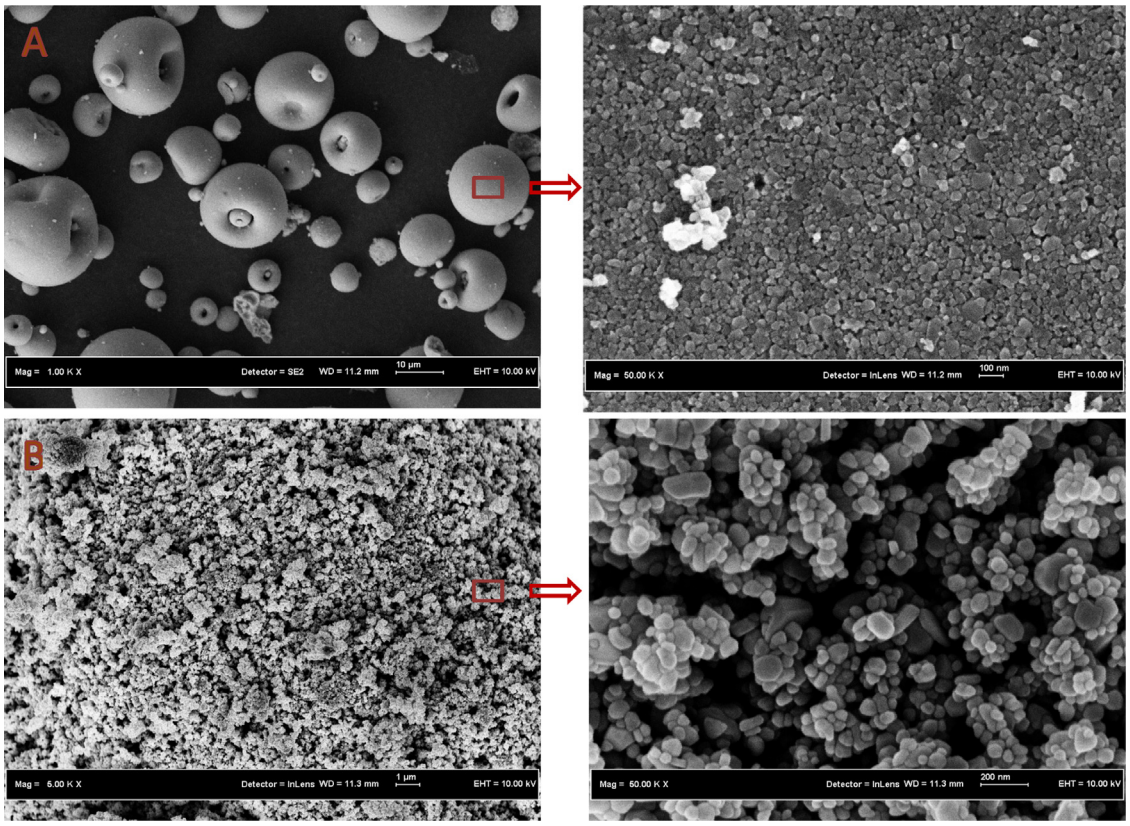

Fig. 1 – FESEM images of feedstock coating powder used; (A) agglomerated nanostructure TiO_2, (B) nanostructure Ag.

material layer [7]. Various types of coating materials have been developed on metallic implant surface, but ceramics shown a better osteoconductivity and excellent mechanical properties, such as calcium phosphate based materials, titanium alloys, and silica based glasses [8–10]. Titanium alloys especially titanium dioxide (TiO_2) have been given great attention because it gathers few superior properties as a thin film coating. In addition of its good corrosive wear resistance, it is also good in enhanced osteoblast adhesion, proliferation and differentiation [11]. Coating CoCr alloy implant with bioactive ceramics of TiO_2 could be a best way to incorporates superior mechanical properties of CoCr alloy with highly biocompatible surfaces.

However, TiO_2 coating alone is insufficient to prevent prostheses surface from bacterial infection. In order to prevent microbial infection in orthopaedic, combination with antibacterial materials is necessary. Silver and its complexes have been found as efficient agent for antibacterial purposes for centuries [12]. Compare to other metals, silver has an advantage of biocompatible with human body and significantly sensitive for microorganisms [13]. Recently, due to high specificity and large specific surface area (SSA), nanoscale size of metallic materials has attracted great attention as they offer better surrounding responses [14]. In vitro studies proved that nanosized ceramics coating enhance mechanical properties, improve cell proliferation and show better antibacterial properties, over coatings from corresponding conventional powders [15,16].

Thus, this study is aimed to deposit nanostructure titanium dioxide-silver on CoCr alloy by using both air plasma spray and high velocity oxy-fuel coating method. The morphology and performance of the coated sample were evaluated.

2. Experimental procedure

2.1. *Experimental materials*

The sprayable feedstock of 99.9% agglomerated nanostructured titanium oxide (TiO_2) and 99.9% silver (Ag) nanopowder were purchased from Inframat Advance Materials, Inc. Fig. 1A shows the nanostructured TiO_2 feedstock. It is observed that each feedstock particle of TiO_2 is formed by an agglomeration of various individual nanosized particles of TiO_2. The nanosized TiO_2 particles are seed-shaped with diameter around 50–100 nm, while the particle size distribution of the feedstock is within 5–50 µm. Fig. 1B shows the distribution of Ag nanopowder with diameter ranging from 40 to 90 nm.

2.2. *Preparation of specimens*

ASTM F1537 standard bulk of cobalt chromium alloy (CoCr alloy) was used in this study, with the alloying elements of 63 wt% Co, 28 wt% Cr, 6 wt% Mo, 1 wt% Si, 1 wt% Mn, and minimum amount of Fe, C, and Ni. The samples were cut into the size of 20 mm × 10 mm × 5 mm, and then mechanically ground and polished using silicon carbide abrasive paper down to 4000 grit. Then, the specimens were extensively cleaned with acetone in the ultrasonic bath for not less than

Table 1 – APS and HVOF parameters.

APS parameters[a]		HVOF parameters[b]
Electric current (A)	300	O_2 flowrate (l/min)
Powder feed rate (g/min)	20	Fuel flowrate (l/min)
Carrier gas flowrate (l/min)	40	Air flowrate (l/min)
Primary gas pressure – Ar (psi)	80	Carrier gas N_2 (l/min)
Secondary gas pressure – H_2 (psi)	50	Spray distance (mm)
Spray distance (mm)	80	Coating layer
Coating layer	5	

[a] SG-100 Plasma Torch.
[b] Diamond Jet Gun.

15 min. The specimens were blasted using aluminium oxide to get about 4.5–5.0 μm of average roughness. Finally, coating was deposited on the substrate by using SG-100 Plasma Torch (Praxair) and Diamond Jet Gun (Sulzer Metco). Table 1 shows the coating parameter for both APS and HVOF coating process.

2.3. *Microstructure and phase characterization*

Zeiss field emission scanning electron microscopy (FESEM) equipped with energy dispersive spectroscopy (EDS) was used to characterize the morphology and elemental analysis of coated specimens. X-ray diffraction (XRD, Siemens-D5000, Germany) with Cu Kα radiation (λ = 1.5405 Å) generated at 35 kV and 25 mA was used to investigate the phase constitutes in as-fabricated coatings. The coatings were directly measured under XRD without polishing. Surface roughness evaluation was carried out by using Mitutoyo SurfTest roughness tester (Mitutoyo, Japan). Porosity of the coating were measured using Dewinter Material Plus software from SEM images of the coating's cross section from different locations. At least five images per sample were analyzed.

2.4. *Mechanical and wear performance*

The hardness of the coating was evaluated by means of conventional tests employing a Shimadzu Vickers Micro-hardness under indentation load of 4.903 N. Pull-off adhesion test was carried out utilizing Defelsko positest AT (ASTM-D4541), where the dollies, 10 mm in diameter, were used. The friction and wear analysis of coating layer were conducted on a pin on disc tester (DUCOM TR-20-M-106) at room temperature (ASTM G99-05) [17]. The equipment allows to have a sliding contact between the 20 × 10 mm area of coating surface and the SS304 disc at a constant rotation speed of 250 r/min, a constant radius of 100 mm, and a constant normal load of 1 kg for total distance of 2000 m under dry conditions. A load cell located at the end of specimens arm holder allows to measure the friction force. The friction force, wear, and time were stored automatically by using data acquisition system. After each wear test, the mass loss of the sample was measured using precision weight balance up to an accuracy of 10^{-4} g. The observation of the worn surface was performed using an optical microscope (OM) and spectroscopy emission microscope (SEM). The wear rates were evaluated in terms of volume loss, while the coefficient of friction was determined by dividing the frictional force by normal load.

3. Results and discussion

3.1. *Coating characterization*

Differences of chemical phases between the initial powder and the coating layer were detected, as indicated in Fig. 2. Consequently, the tetragonal phase transformation of TiO_2 often occurs during high-temperature service process conditions, which results in a significant density drop of up to 8% [18].

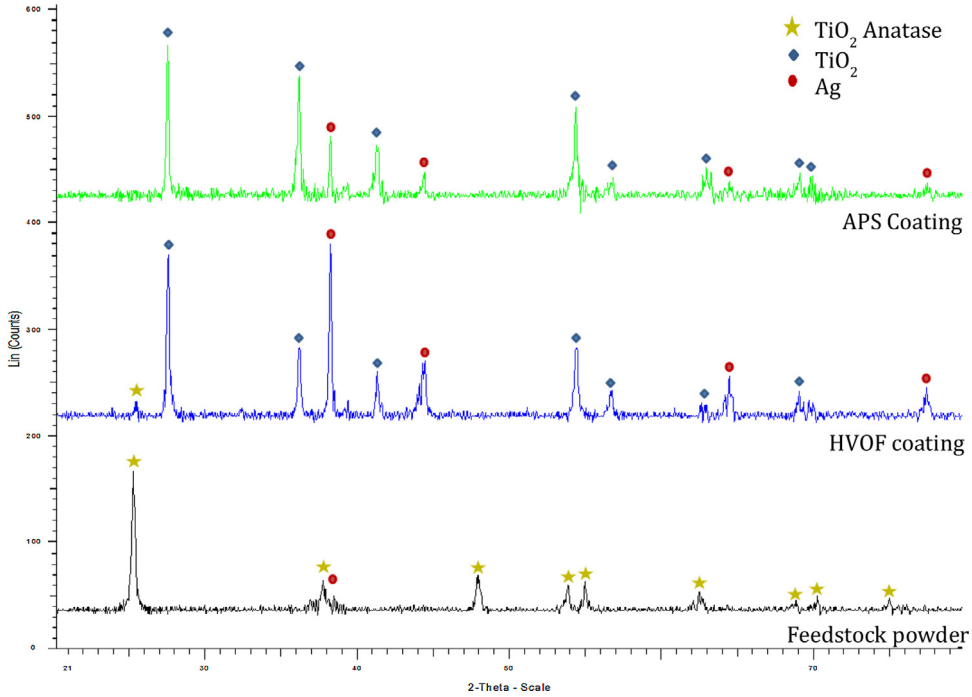

Fig. 2 – XRD pattern for feedstock powder, APS sprayed and HVOF sprayed nanostructure TiO_2–Ag.

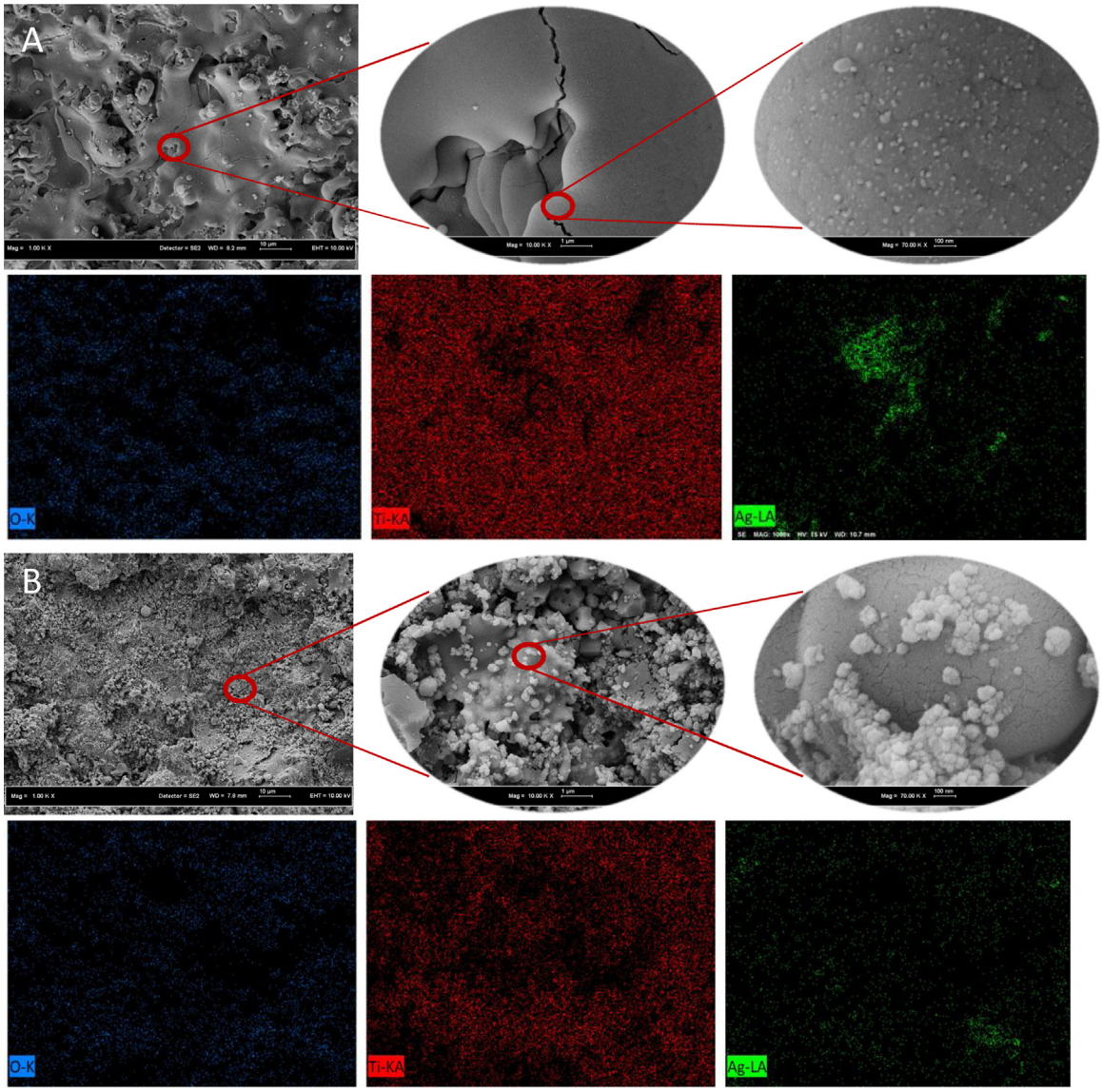

Fig. 3 – FESEM image together with elemental mapping of nanostructure TiO_2–Ag coating on CoCr alloy; (A) APS sprayed, (B) HVOF sprayed.

The density reduction could generate thermal stresses and eventually result in degradation and failure of the coatings [19]. According to XRD patterns shown, rutile TiO_2 phase was present in both the as-sprayed coatings while low peak of anatase phase was detected only in HVOF coating. The formation of rutile phase is due to the high gas temperature during deposition process [20], which high plasma temperature of APS process was fully transformed anatase phase into rutile, while it was partially transformed in HVOF sprayed coating. On the other hand, no significant chemical reaction and degradation detected between the two elements of the sprayed powders (TiO_2 and Ag). These pattern corresponded to the anatase phase of TiO_2 (JCPDS Card No. 21-1272), rutile phase of TiO_2 (JCPDS Card No. 21-1276), and Ag (JCPDS Card No. 04-0783).

EDX mapping analysis in Fig. 3 reveals that coating powder was differently melted for both coating technique. More melted splats can be seen in APS sprayed compare to HVOF sprayed nanostructure TiO_2–Ag. In addition, both coatings exhibited different silver distribution, where silver was splotchy distributed in APS coating while uniformly distributed in HVOF coating. It is widely known that the intermolecular force procedure of thermally sprayed silver particles is isolated and their attraction to each other terminated before the impingement on substrate surface. The cohering process in APS coating technique can be treated as impact of melted particle upon solid surface. Considering the composite coating formation succeed, it can be assumed that the velocity of the particle at the end of the impact approaches zero, particularly, no rebounding took place.

Reduced amount of the micro-cracks is observed in HVOF coatings, where unmelted particles play roles in stop the growth of nano-cracks, which help to prevent the formation of micro-cracks. Fig. 4 shows the cross section of the coating

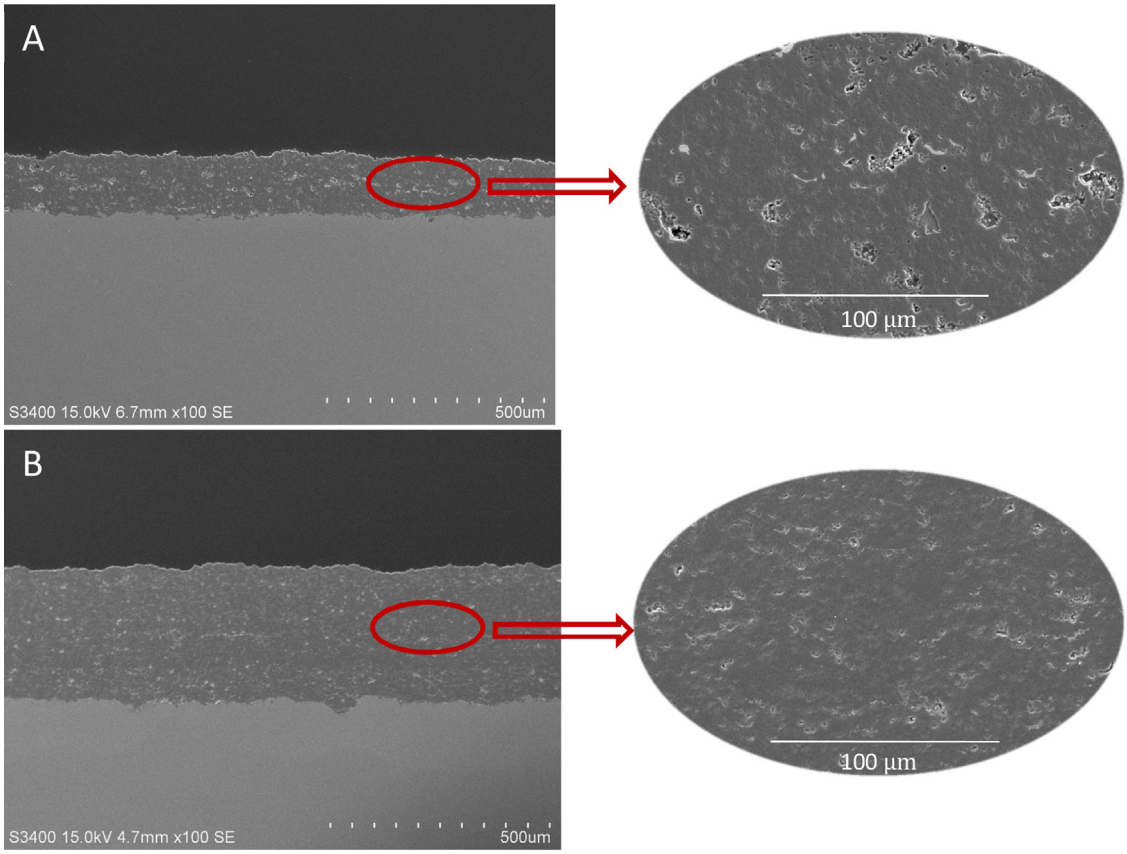

Fig. 4 – Cross-section of nanostructure TiO_2–Ag coating on CoCr alloy; (A) APS sprayed, (B) HVOF sprayed.

samples. The interface between coating and substrate exhibits less oxide and no visible delamination and cracks. The HVOF coating shown a slightly larger thickness per spray layer than that of the APS coating. This can be partially attributed to the relatively higher feed rate of HVOF coating process.

For both coatings techniques, there is no obvious stratification and big pores found. It is possible to discover that the nanostructure TiO_2–Ag coating microstructure is relatively denser and homogeneous. The average porosity of the coatings measured from was found to be below 10%, which are almost in agreement with the findings of Dwi Bayuwati [20]. This finding shows that particles with high temperature and jet speed would create adequate splat formation after the contact on the substrate, which results in isotropic "bulklike" microstructure and high density. However, much more porosities can be found in the APS sprayed nanostructure TiO_2–Ag coating than those in the HVOF sprayed coating.

3.2. *Microhardness*

Table 2 concluded the properties of APS and HVOF sprayed nanostructure TiO_2–Ag coatings. As expected, the porosity values has a strong relationship with microhardness of the coatings. The microhardness was discovered to be high as the porosity level is low. The higher hardness of the HVOF coating compared to the APS coating can be attributed to the high particle velocity, the low porosity with dense coating. This kind of microhardness is in consistent with previous investigations [21], although slightly lower than plasma spray TiO_2 coating reported by Forghani et al. [22]. It was expected that addition of Ag in the coating reduce their mechanical strength. It was reported that mechanical performance of alloy will be increased by small additions of 0.5 up to 1 wt.% of Ag [23], however, further increase of Ag content will reduce the strength due to the inherent incompatibility between the particles and the alloy matrix during deformation [24].

Table 2 – Properties of APS and HVOF sprayed nanostructure TiO_2–Ag coating on CoCr alloy.

Properties	APS coating	HVOF coating
Microhardness (Hv)	500.0	528.0
Adhesion strength (MPa)	20.84	23.38
Porosity (%)	9.0	8.1
Roughness (µm)	4.51	5.35
Thickness/layer (µm)	29.58	31.95

The enhanced microhardness of the coatings deposited by APS and HVOF also can be associated to the improved splats formation and bonding, in other word, a role of the degree of melting and velocity of the droplets during deposition course. In addition, it has been revealed that TiO_2 coating layers comprised of two phases, and the resultant microhardness value of the coating layer delicately varies based on the fraction phases. Previous studies on the properties of resultant phases in TiO_2 ceramic [25] has shown that the microhardness of

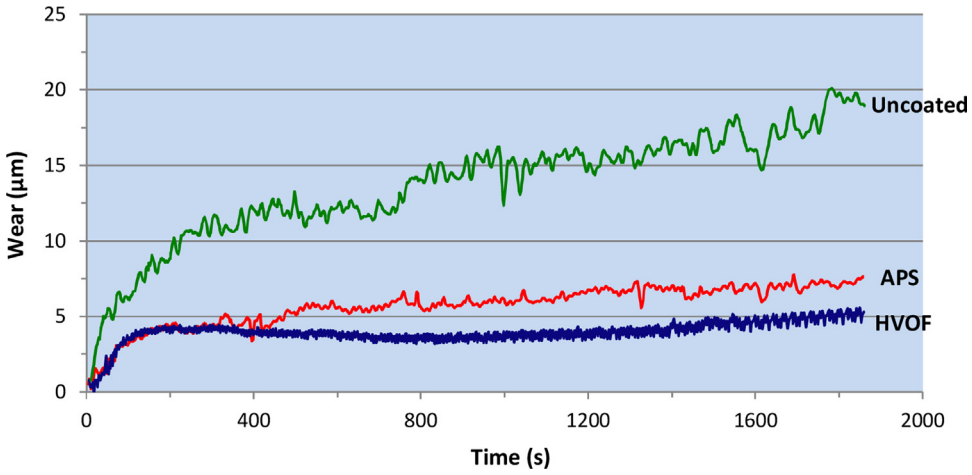

Fig. 5 – Wear behaviour of the coated and uncoated samples in the function of time.

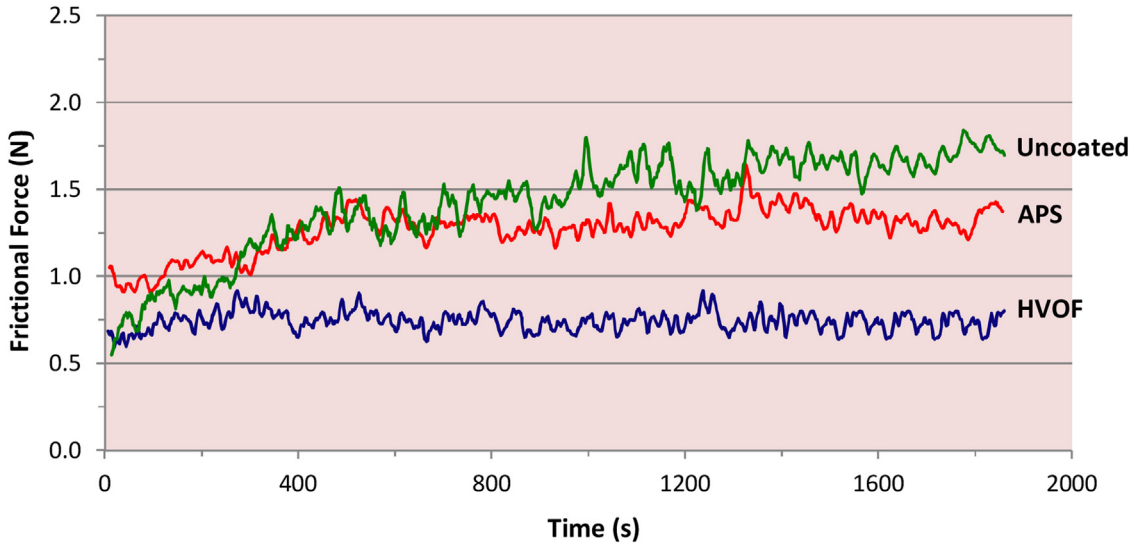

Fig. 6 – Frictional force of the coated and uncoated samples in the function of time.

the anatase and rutile, respectively. Consequently, the resultant microhardness in a present of anatase peak intensity is favourably higher, and this correlation of the microhardness value with the phase ratio confirm the possible phase revolution during the deposition process.

3.3. *Adhesion strength*

The adhesion strengths results of more than 20 MPa were achieved for both thermal spray coatings obtained in this study, which was summarized in Table 2. The HVOF sprayed nanostructure TiO_2–Ag coating exhibited an adhesion strength 10% higher than the adhesion strength of the APS coating. It has been reported in the literature that HVOF coatings tend to exhibit higher adhesion strength results than those of APS coatings [26]. Lower porosity level attained by the HVOF coating when compared with APS coating are probably the factor attributed to the higher values of adhesion strength. In addition, macroscopic and microscopic thermal stress that resulted from different in thermal expansion coefficient between the coating powder and substrate surface, and deposition of high temperature splats onto cold substrate also contribute to weaken the adhesion strength. Due to close thermal expansion coefficient between ceramic TiO_2 and CoCr alloy, hence would not trigger the formation of significant macroscopic thermal stress. However, microscopic stresses occur within the high temperature sprayed particles onto a cold substrate, with the higher thermal, the larger the quenching stresses. This explain that the residual stress arises in APS process is probably higher than in HVOF process with similar feedstock particles. It is important to point out that both adhesion strength of thermal sprayed TiO_2 coatings is lower than those reported in literature [27]. This weaker strength could be attributed to the addition of Ag, where apparently no chemical reaction developed between Ag and TiO_2, and low mechanical properties of Ag.

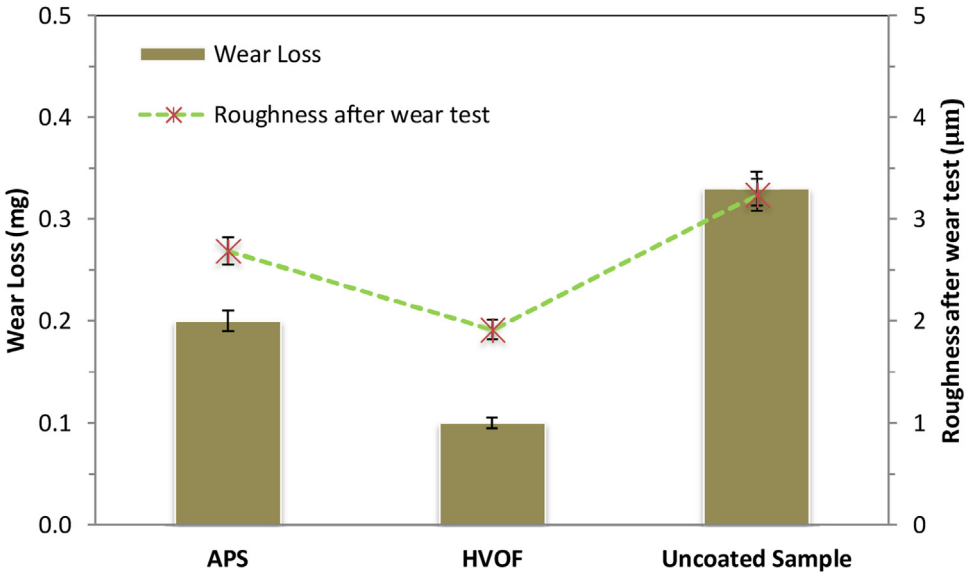

Fig. 7 – Average wear loss and surface roughness for APS TiO_2–Ag coated, HVOF TiO_2–Ag coated and uncoated CoCr alloy sample after pin-on-disc test.

3.4. *Wear and friction behaviour*

As shown in Fig. 5, under dry conditions, the wear rate of APS and HVOF sprayed nanostructure TiO_2–Ag coatings is lower than bare CoCr alloy sample. This phenomena was attributed by hard nano-scale reinforcements embedded in nanostructure TiO_2–Ag thin film, which help to prevent the direct contact between substrate material and counterpart material. It explained the effect of hardness on the wear behaviour of the material. The wear rate of the coatings was highly accelerate for the first 2 min of sliding time and then steadily increase after that. This is believed that it happened due to the run-in. In this period, during the contact between the rough surface of nanostructure TiO_2–Ag composite coating and the hard SS304 disc, there was a strong tendency to asperity breaking. Thus an extensive initial wear occur by breaking of the asperity peaks, which then smoothing the coatings surface. In comparison to the sliding time of first 2 min, for the rest of sliding time, the surface texture of the contact zone turned smoother due to the shift from run-in period to the stable-wear period.

On the other hand, a slow down in wear rate of the coatings after certain time of sliding also could be attributed to the formation of plastically deformed TiO_2–Ag nanoparticles, separated from matrix due to abrasion, sheering, breakage, or peening-over, on the disc and coating surface. For this situation, the shearing stress which generates resistance to motion, act as solid lubricants between two sliding surfaces. As asperities were broken off, it leads in spattering and patching of nanostructure TiO_2–Ag debris on some parts of the sliding wear track, which can be speculated that it was responsible for decreasing the wear rate of samples. According to Zhu et al. [28], wear is influenced by the loss flux of the depletion particle and the worn particle detached in between the sliding surfaces is favourable in wear system. The high formation rate of detached coating material in two sliding surfaces will reduce the wear rate, in condition that the detached particles stay in the contact area. Due to its high microhardness and toughness, the TiO_2 coating is hardly delaminated under the shear stress, which means that the formation rate of detached material is low. Rather than release as flakes, the stucked detached material transforms to a displacement layer under the cyclic flow, evidenced by the wear versus time graph shown, where the slightly decrease in wear rate is observed. Thus, the wear behaviour in sliding surfaces is sensitively affected by the ejection of detached material.

Fig. 6 shows the frictional force of the coated and uncoated samples sliding against SS304 disc. It can be observed that HVOF sprayed coating sample possesses the lowest frictional force (0.57–0.94), while APS sprayed coating and uncoated samples have a slightly higher frictional force (1.22–1.85 and 0.51–1.78) than HVOF sprayed coating. These frictional force and wear characteristic are identical to the microstructure as well as porosity and mechanical properties of the coatings. Specifically, lots of micro-cracks and pores between deposited partially molten particles in APS sprayed coating, contribute to noticeable reduction of toughness, which more simply removed during abrasion and sheering; while, the low microhardness can induce much deeper furrows to be produced on the sliding surfaces under the similar wear test conditions, which can increase the frictional force of two sliding parts [29]. Differ from APS sprayed coating, denser deposited partially molten particles in HVOF sprayed coating are more difficultly delaminated during pin-on-disc tests, in contrast, the higher microhardness of the coating layer can prevent the formation of furrows, thus contribute to lower frictional force. The much severe delamination of coating particles and deeper furrows cause greater severe fatigue and abrasive wear for APS sprayed coatings, resulting in higher wear rates. It can be said that the microstructure and mechanical behaviour of thermally deposited coatings play a greater role in control their wear resistance.

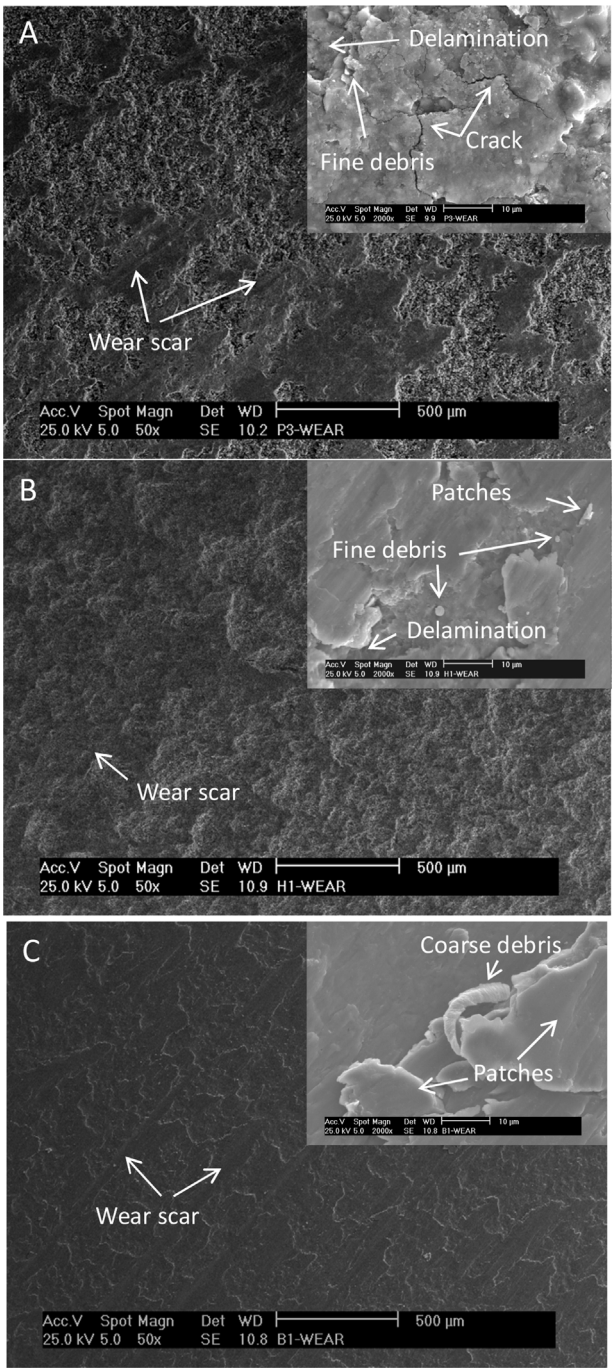

Fig. 8 – SEM images of wear track of (A) APS TiO_2–Ag coated, (B) HVOF TiO_2–Ag coated and (C) uncoated CoCr alloy sample.

Although there is a slight increase in frictional force for APS and HVOF sprayed coatings at early stage, due to high roughness of the coating surface, but it still can be consider stable. This stability could be attribute to the plastically deformed asperity peaks, which help to enhance smoothness between two sliding surface. On the other hand, the frictional force of bare CoCr alloy was started with lowest value, which probably because of polished surface of the sample. In the meantime, as the frictional force increased it was resulting in the increase of surface roughness. This mechanism could be explained more by the wear loss and surface roughness of the samples after pin-on-disc wear test as shown in Fig. 7. It indicates that the roughness of the coated samples were reduced down to 2.681 μm for APS sprayed coating and 1.919 μm for HVOF sprayed coating, while the roughness of uncoated sample was increased to 3.241 μm. Besides that, HVOF sprayed coating shown lowest wear loss, followed by APS sprayed coating and bare CoCr alloy. The wear loss and surface roughness results are in favour of frictional force and wear data of the samples.

This wear behaviour of the coatings could be explained with respect to the scanning electron micrographs images of worn surfaces. The SEM of the worn coating surface and uncoated surface after 200 m of contact distance are shown in Fig. 8(A)–(C) respectively. Various zone and wear tracks are

Table 3 – Surface EDS analysis of bare, plasma sprayed and HVOF sprayed CoCr alloys before and after wear test.

Samples		Mass fraction, %					
		Co	Cr	Mo	Ti	O	Ag
Bare	Before	51.80	29.04	19.16	–	–	–
	After	43.96	47.15	5.04	–	3.86	–
Plasma sprayed	Before	–	–	–	60.80	36.78	2.42
	After	–	2.77	–	50.60	37.26	2.77
HVOF sprayed	Before	0.36	1.16	–	59.13	36.55	2.80
	After	4.14	1.74	–	56.35	33.85	2.88

observed in the image. Some prows were formed on the coatings worn surface while some regions were protruded. The sliding tracks of worn surface on APS and HVOF coatings had a dark texture and scratches parallel to the direction of motion were observed, which are well correspond to abrasive wear as it was also detected on bare CoCr alloys. Due to repeatedly high contact stresses and frictional heating over the surface, discontinuity of the patches and generation of fine spherical particles detected. There were some dispersed particles throughout the worn surface of nanostructure TiO_2–Ag composite coating. The high magnification SEM images reveals a large amount of plastic deformation occurred on the worn surface of bare CoCr alloys, indicated by microcracks and wears debris (Fig. 8C). Meanwhile, the amount of plastic deformation and scuffing wear were reduced for both the APS and HVOF sprayed coating. The reduction of plastic deformation corresponding to APS and HVOF sprayed coating was associated to the strengthening tune up effect resulted from compact nanostructure that interfered the dislocations movements in the metallic matrix of the composite coatings.

It shows that the surface of the HVOF sprayed nanostructure TiO_2–Ag has smaller wear scar without cracks than that of APS coating, while both coatings show the less damage suffered. There was no presence of any other elements detected by EDS analysis, as shown in Table 3. The reason why the HVOF sprayed coating presents better performance in a pin-on-disc wear test compare to APS sprayed coating can be clarified by its mechanical properties. In comparison to the APS sprayed coating, the HVOF sprayed coating is harder and lower porosity, and the detachment of coating particles is slower. Thus, wear characteristic is strongly depend on the both material's mechanical properties and microstructure. For bare CoCr alloy sample, the scar is deeper and clearly visible, while the worn debris produced is bigger than those in coated samples. These phenomena is attributed to the nanoscale of the TiO_2–Ag particles in both coated samples. The deliminated particles from its matrix due to wear mechanism is in nanosize, which minimize the effect of debris on two interacting surface. This is very beneficial in tribological system based application.

4. Conclusion

In this work, TiO_2–Ag nanocomposite coatings with high hardness and wear resistance compared with bare CoCr alloys have been successfully obtained by thermally deposited of nanostructured TiO_2 dispersed particles with Ag. The following conclusions can be drawn from the present investigation:

- XRD characterization of the coatings revealed the phase changes from the primary TiO_2 powder's phase composition, while no chemical reaction occurred between TiO_2 and Ag. Rutile TiO_2 phase was fully transformed into anatase in APS coating while partially transformed in HVOF coating. Hence, it is believed that differences of microstructure and properties of the engineered coatings observed in this work were strongly associated to the differences in the degree of particle melting and velocity.
- By comparatively it was found that HVOF sprayed TiO_2–Ag nanocomposite coating showed a better microhardness and adhesion strength compare to APS sprayed TiO_2–Ag nanocomposite coating, however, the values obtained were lower than those generally found in the literature for thermally sprayed TiO_2 coatings, which suggest that the addition of Ag affect the properties of coatings.
- The frictional force of nanostructure TiO_2–Ag coating is smaller for both APS and HVOF sprayed as compared with bare CoCr alloy, proving an enhancement of wear resistance.
- The dimension of the wear track and number of wear crack corresponding to HVOF sprayed TiO–Ag composite coating is lesser than that of the APS sprayed. Wear performance of the coating is highly affected by its microhardness and porosity.

Conflicts of interest

The authors declare no conflicts of interest.

Acknowledgements

The authors wish to place their sincere thanks to the Malaysian Ministry of Higher Education for financial support of the Fundamental Research Grant Scheme (FRGS, No. FRGS/1/2015/TK03/UTM/01/3). The authors also wish to acknowledge all those involved for valuable support provided during this work.

The authors are grateful to the editor and reviewers for valuable technical advice and kind help in improving the language skills of the paper.

REFERENCES

[1] Bauer S, Schmuki P, von der Mark K, Park J. Engineering biocompatible implant surfaces. Prog Mater Sci 2013;58(3):261–326.

[2] Wang Q, Zhang L, Dong J. Effects of plasma nitriding on microstructure and tribological properties of CoCrMo alloy implant materials. J Bionic Eng 2010;7(4):337–44.
[3] Hansen DC. Metal corrosion in the human body: the ultimate bio-corrosion scenario; 2008.
[4] Delaunay C, Petit I, Learmonth ID, Oger P, Vendittoli Pa. Metal-on-metal bearings total hip arthroplasty: the cobalt and chromium ions release concern. Orthop Traumatol Surg Res 2010;96(8):894–904.
[5] Day JS, Baxter RM, Ramsey ML, Morrey BF, Connor PM, Kurtz SM, et al. Characterization of wear debris in total elbow arthroplasty. J Shoulder Elb Surg 2013;22(7):924–31.
[6] Wang L-N, Luo J-L. Preparation of hydroxyapatite coating on CoCrMo implant using an effective electrochemically-assisted deposition pretreatment. Mater Charact 2011;62(11):1076–86.
[7] Nagarajan S, Rajendran N. Surface characterisation and electrochemical behaviour of porous titanium dioxide coated 316L stainless steel for orthopaedic applications. Appl Surf Sci 2009;255:3927–32.
[8] Dorozhkin SV. Calcium orthophosphate coatings, films and layers. Prog Biomater 2012;1(1).
[9] Serro AP, Completo C, Colaço R, Santos F, Lobato C, Cabral JMS, et al. A comparative study of titanium nitrides, TiN, TiNbN and TiCN, as coatings for biomedical applications. Surf Coat Technol 2009;203(24):3701–7.
[10] Ruan J, Wang K, Song H, Xu X, Ji J, Cui D. Biocompatibility of hydrophilic silica-coated CdTe quantum dots and magnetic nanoparticles. Nanoscale Res Lett 2011;6(1):299.
[11] Tan AW, Pingguan-Murphy B, Ahmad R, Akbar SA. Review of titania nanotubes: fabrication and cellular response. Ceram Int 2012;38(6):4421–35.
[12] Devrim K, Özalp H, Attar A, Sargon MF. Nanoparticle silver ion coatings inhibit biofilm formation on titanium implants. J Clin Neurosci 2011;18(3):391–5.
[13] Fordham WR, Redmond S, Westerland A, Cortes EG, Walker C, Gallagher C, et al. Silver as a bactericidal coating for biomedical implants. Surf Coat Technol 2014;253:52–7.
[14] Das G, Dutta R, Gogoi P, Buragohain AK, Karak N. Antibacterial activities of copper nanoparticle-decorated organically modi fi ed montmorillonite/epoxy nanocomposites. Appl Clay Sci 2014;90: 18–26.
[15] Yilmaz O, Yorgancioglu A. Nanocoatings: preparation, properties, and biomedical applications. In: Vasile C, editor. Micro and nano technologies, polymeric nanomaterials in nanotherapeutics. Elsevier; 2019. p. 299–331.
[16] Achanta J-PCS, Drees D. Nanocoatings for tribological applications. In: Abdel Salam Hamdy Makhlouf I, Tiginyanu, editors. Metals and surface engineering, nanocoatings and ultra-thin films. Woodhead Publishing; 2011. p. 355–96.
[17] Parthasarathi NL, Duraiselvam M, Borah U. Effect of plasma spraying parameter on wear resistance of NiCrBSiCFe plasma coatings on austenitic stainless steel at elevated temperatures at various loads. Mater Des 2012;36:141–51.
[18] Bannier E, Darut G, Sánchez E, Denoirjean A, Bordes MC, Salvador MD, et al. Microstructure and photocatalytic activity of suspension plasma sprayed TiO_2 coatings on steel and glass substrates. Surf Coat Technol 2011;206(2–3):378–86.
[19] Ganvir A, Curry N, Markocsan N, Nylén P, Toma F. Comparative study of suspension plasma sprayed and suspension high velocity oxy-fuel sprayed YSZ thermal barrier coatings. Surf Coat Technol 2015;268:70–6.
[20] Bayuwati D. Structural and morphological characteristics of plasma sprayed TiO_2-coatings. Indones J Mater Sci 2012;14(1):18–23.
[21] Wojciech Z, Kozerski S. Scuffing resistance of plasma and HVOF sprayed $WC_{12}Co$ and $Cr_3C_{2\text{-}25}$ ($Ni_{20}Cr$) coatings. Surf Coat Technol 2008;202:4453–7.
[22] Forghani SM, Ghazali MJ, Muchtar A, Daud AR, Yusoff NHN, Azhari CH. Effects of plasma spray parameters on TiO_2-coated mild steel using design of experiment (DoE) approach. Ceram Int 2013;39(3):3121–7.
[23] Choi HW, Choi JH, Lee KR, Ahn JP, Oh KH. Structure and mechanical properties of Ag-incorporated DLC films prepared by a hybrid ion beam deposition system. Thin Solid Films 2007;516(2–4):248–51.
[24] Song M, Chen KH, Huang LP. Effects of Ag addition on mechanical properties and microstructures of Al–8Cu–0.5Mg alloy. Trans Nonferrous Met Soc China (English Ed) 2006;16(4):766–71.
[25] Podlesak H, Pawlowski L, Laureyns J, Jaworski R, Lampke T. Advanced microstructural study of suspension plasma sprayed titanium oxide coatings. Surf Coat Technol 2008;202(15):3723–31.
[26] Liu Y, Fischer TE, Dent A. Comparison of HVOF and plasma-sprayed alumina/titania coatings – microstructure, mechanical properties and abrasion behavior. Surf Coat Technol 2003;167:68–76.
[27] Lima RS, Marple BR. From APS to HVOF spraying of conventional and nanostructured titania feedstock powders: a study on the enhancement of the mechanical properties. Surf Coat Technol 2006;200:3428–37.
[28] Zhu X, Lauwerens W, Cosemans P, Van Stappen M, Celis JP, Stals LM. Different tribological behavior of MoS_2 coatings under fretting and pin-on-disk conditions. Surf Coat Technol 2003;164:422–8.
[29] Hou G, An Y, Zhao X, Zhou H, Chen J. Effect of critical plasma spraying parameter on microstructure and wear behavior of mullite coatings. Tribiol Int 2016;94:138–45.